



# Anti-Diabetic Activity of Silver Nanoparticles Synthesized from the Hydroethanolic Extract of *Myristica fragrans* Seeds

Ramya Perumalsamy<sup>1</sup> · Lavanya Krishnadhas<sup>1</sup>

Received: 6 July 2021 / Accepted: 21 January 2022

© The Author(s), under exclusive licence to Springer Science+Business Media, LLC, part of Springer Nature 2022

## Abstract

*Myristica fragrans*, also known as nutmeg, is a spice that cures various diseases. This study aimed to synthesize silver nanoparticles from a hydroethanolic extract of *Myristica fragrans* seeds (MFHE) and evaluate their anti-diabetic properties. To MFHE, AgNO<sub>3</sub> solution was added and exposed to sunlight to produce silver nanoparticles from hydroethanolic seed extract of *Myristica fragrans* (MFHENP). The MFHENP was characterized by numerous techniques. UV-visible spectroscopy confirmed the formation of silver nanoparticles by the absorption peak at 430nm. Scanning electron microscopy (SEM) studies revealed the shape and size of the particles at the range of 50–60nm. Energy-dispersive X-ray spectroscopy (EDX) disclosed the presence of silver ions. X-ray diffraction spectrum confirmed the crystalline nature of silver nanoparticles by the peak at 39°. FTIR analysis revealed the functional groups present in MFHE as well as in MFHENP and zeta potential analysis was found to be 14mV. Furthermore, in vitro anti-diabetic activity was investigated. MFHENP showed significant efficiency against the inhibition of alpha-amylase and alpha-glucosidase enzymes and also MFHENP retarded the glucose transport across the membrane which is analyzed by glucose diffusion and glucose uptake assays. Acarbose is used as a standard for all these methods and MFHENP efficiency proves their therapeutic potential for the treatment of diabetes mellitus.

**Keywords** Diabetes mellitus · *Myristica fragrans* · Silver nanoparticles · Characterization · Anti-diabetic activity

## Introduction

Nanoscience is the analysis of structures and molecules on nanometer scales ranging from 1 to 100 nm, whereas nanotechnology is the study that applies nanoscience to practical applications such as computers. Nanotechnology is one of the most enticing twenty-first-century innovations. Several studies have demonstrated the enormous potential of nanotechnologies in biomedicine for the diagnosis and treatment of a wide range of human

---

✉ Ramya Perumalsamy  
ramyamiya11@gmail.com

<sup>1</sup> Department of Biochemistry, PSG College of Arts & Science, Coimbatore, Tamil Nadu 641014, India

diseases [1]. Silver nanoparticles (AgNPs) are crucially significant in nanomedicine because of their appealing physicochemical properties, high antimicrobial capability and low toxicity, specific capacity to establish versatile nanostructures, and low manufacturing costs [2]. Compared to other metal nanoparticles such as gold, zinc, and copper, silver nanoparticles are far less toxic to mammalian cells. Green synthesis is a technique for the synthesis of nanoparticles that has exploded in popularity in recent years due to its protection, effectiveness, and low cost [3]. Nanotechnology has been particularly important in the diagnosis and treatment of diabetes in the past few years. It also has a clear track record for detecting and treating diabetic complications [4].  $\alpha$ -amylase and  $\alpha$ -glucosidase are key enzymes, which break down the carbohydrates into monosaccharides which is a reason for increased blood sugar. Silver nanoparticles bind to these enzymes and inhibit their reactions in signaling pathways. So the blood sugar levels are decreased [5].

Diabetes affects approximately 422 million people worldwide, the majority of whom live in low- and medium-income nations, and diabetes is directly responsible for 1.6 million deaths worldwide in a year [6]. Diabetes mellitus is a chronic condition that emerges when the pancreas fails to generate adequate insulin or when the body's insulin is ineffectively used. Insulin is a hormone that helps to keep blood sugar levels in check [7]. Type I and type II diabetes are characterized by hyperglycemia (high level of blood sugar), which can lead to severe health problems. Gestational diabetes occurs when glucose intolerance manifests as hyperglycemia of varying severity and begins during pregnancy [8]. Anti-diabetic medications such as acarbose, voglibose, metformin, and gliclazide work by suppressing the enzymes, but they have severe side effects such as diarrhea, bloating, and distention [9]. Medicinal plants and spices are natural antioxidants and herbal medicines, owing to anti-diabetic compounds which enhance pancreatic tissue function [10]. As a result of their low cost, wide availability, and lack of side effects, herbal products have become increasingly popular in the management of diabetes [11].

*Myristica fragrans*, also known as nutmeg, reside in the Myristicaceae family. It produces both nutmeg and mace, which are both economically important spices. Nutmeg is primarily grown in southern India, especially in Tamil Nadu. Since the Middle Ages, nutmeg has been used as a folklore remedy to treat a variety of ailments, including stomach, appetite stimulant, diarrhea, and flatulence regulation [12]. Plant constituents present in *Myristica fragrans* are myristicin, elemicin, eugenol, dehydrodiisoeugenol, and myristic acid. Recent studies on nutmeg exert many pharmacological activities such as anti-inflammatory, antipyretic, anthelmintic, digestive, antispasmodic, narcotic, anticonvulsant, antiseptic, constipating and tonic, antihepatotoxic, anticancer, antidepressant, hypolipidemic, and antifungal [13]. With this knowledge, the research has been focused on the synthesis of silver nanoparticles from *Myristica fragrans* seed extract and the subsequent evaluation of their in vitro anti-diabetic activity.

## Materials and Methods

### Plant Collection and Extraction

Seeds of *Myristica fragrans* were collected from the Kallar Garden, Mettupalayam, Coimbatore. Authentication was done at the Botanical Survey of India at TNAU Coimbatore district, India (BSI/SRC/5/23/2021/Tech/142). The collected seeds were washed thoroughly in tap water, shade-dried, and powdered. Twenty grams of powder was dissolved in 200ml

of hydroethanol solvent and the mixture was kept in a shaker for 72 h. This extract was filtered using cheesecloth and the filtrate was stored in refrigerator condition.

## Synthesis of AgNPs

Five hundred milliliters of 1mM silver nitrate ( $\text{AgNO}_3$ ) was prepared using double-distilled water. To 50ml of the hydroethanolic extract of *Myristica fragrans* seeds (MFHE), 450ml of 1mM  $\text{AgNO}_3$  solution was added. The hydroethanolic extract of *Myristica fragrans* seeds with silver nitrate solution (MFHENP) was exposed to sunlight for 20 min [14]. The appearance of dark brown color indicates the formation of silver nanoparticles. The synthesized AgNPs were separated by centrifugation at 5000rpm for 15 min. Colored supernatant solutions were obtained by repeating the procedure with pellets dispersed in water. The sample was dried, then stored at 4°C for further use [15].

## Characterization of AgNPs

### UV-Visible Spectroscopy of MFHENP

UV-visible spectral analysis characterizes the formation and completion of silver nanoparticles. The bio-reduction of  $\text{Ag}^+$  ions to form AgNPs was examined by intermittently measuring the absorption spectra of the reaction solution using a UV-vis spectrophotometer for 24 h between the range of 300 and 800nm. The color of the reaction solution was also recorded at each time interval [16].

### SEM with EDX Analysis of MFHENP

SEM and EDX studies were used to examine the surface morphology and basic compositions of the MFHRNP. The MFHENP was uniformly distributed on the sample holder using carbon tape and sputter coated with platinum using an ion coater system for 120 s before being observed under SEM. After obtaining SEM images, the elemental composition of AgNPs was investigated using an EDX detector connected to the SEM machine [17]. The SEM machine used is TESCAN MIRA3 FEG -SEM.

### XRD Analysis of MFHENP

An XRD spectrum was taken to validate the crystalline structure of the synthesized nanoparticles. It was analyzed using an XRD (SHIMADZU, XRD7000) with K1 Cu radiation and a  $2\theta$  range of 20–80, 30mA current, and 40kV voltage. Using XRD peaks, the crystallographic structure of MFHENP was determined [18].

### FTIR Analysis of MFHE and MFHENP

FTIR analysis was used to evaluate the functional groups present in MFHE and MFHENP. It was used to find the functional groups in plant extracts that were responsible for the reduction of  $\text{Ag}^+$  ions during the synthesis of silver nanoparticles. It was analyzed with a resolution of  $16\text{cm}^{-1}$  and a range of  $4000\text{--}500\text{cm}^{-1}$  [19].

## Zeta Potential Analysis of MFHENP

The stability of AgNPs was studied using zeta potential. The zeta potential measurement was done using a Zetasizer Nano ZS in a disposable cell at 25°C, and the results were analyzed using Zetasizer software. Zeta potential determines the surface potential of silver nanoparticles and it is essential for the characterization of the stability of nanoparticles [20].

## In Vitro Anti-Diabetic Activity

### In vitro $\alpha$ -Amylase Inhibitory Activity

In phosphate buffer, different concentrations of plant extracts were prepared from a 1 mg/ml stock solution. Two hundred to 1000  $\mu$ l of MFHENP extract and acarbose were mixed with 500  $\mu$ l of  $\alpha$ -amylase (0.5 mg/ml) and incubated at room temperature for 10 min. After that, 500  $\mu$ l of 1% starch solution was applied and incubated for the next 10 min. After that, 1 ml of coloring reagent was applied to the reaction mixture and heated for 15 min in a boiling water bath before adding 10 ml of distilled water. To measure the absorbance of the colored extracts, a blank was made by substituting the enzyme with buffer for each concentration of the sample set. At 540 nm, the absorbance was calculated [21].

$$\% \text{inhibition} = (\text{Abs control} - \text{Abs sample} / \text{Abs control}) \times 100$$

### In Vitro $\alpha$ -Glucosidase Inhibitory Activity

To 36  $\mu$ l of phosphate buffer solution, 30 ml of MFHENP solution with different concentrations (200–1000  $\mu$ g/ml) and 17  $\mu$ l of 4-nitrophenyl-D glycopyranoside (PNPG) substrate at 5 mM were heated to 37°C for 5 min. After 5 min, each well received 17  $\mu$ l of  $\alpha$ -glucosidase solution 0.15 U/ml, for a total volume of 100 ml. The reaction was spotted by applying 100  $\mu$ l of sodium carbonate 200 mM to the mixture and incubating it for 15 min. A microplate reader was used to test absorbance at 405 nm [22].

$$\% \text{inhibition} = (\text{Abs control} - \text{Abs sample} / \text{Abs control}) \times 100$$

## Glucose Diffusion Assay

This assay used a dialysis model to determine the diffusion of glucose in the presence of MFHENP by the method of Vani [23]. The dialysis bag was filled with 1 ml of extract and 1 ml of glucose solution (20 mM in 0.15 M NaCl) for the experiment (12000 MW, Hi-Media laboratory). The dialysis bag was wrapped on both ends and put in a 200-ml beaker with 45 ml 0.15 M NaCl. One milliliter of 0.15 M NaCl, 20 mM glucose, and 1 ml distilled water were added to the control bag. The concentration of glucose in the external solution was calculated. At room temperature (202°C), the beaker was put in an orbital shaker. The glucose concentrations were calculated using the O-toluidine procedure.

## Glucose Uptake by Yeast Cells

This assay was carried out according to the method of Abubakar [24] with some changes. To make a 1% suspension, a commercial baker's yeast was dissolved in distilled water. The suspension was stored at room temperature overnight (25°C). The yeast cells samples were centrifuged at 4000 rpm for 5 min the next morning. This method was repeated until a clear supernatant was obtained by adding distilled water to the pellet. To make a 10% v/v suspension of the yeast cells, 10 parts of the clear supernatant fluids were combined with 90 parts of distilled water. The mixture was then mixed with 5mM of 1ml glucose solution and incubated for 10 min at 37°C. To begin the reaction, 100µl of yeast suspension was put into the glucose and extract mixture and incubated at 37°C for 60 min. The tubes were centrifuged for 5 min at 3800 rpm after incubation, and glucose was measured with a spectrophotometer at 520 nm. On the same wavelength, the absorbance of the respective control was recorded. The control solution contains all reagents except the test sample. The formula used to measure the percentage rise in glucose uptake:

$$\%inhibition = (Abs\ control - Abs\ sample / Abs\ control) \times 100$$

## Results and Discussion

### Synthesis of AgNPs

The color transition from yellow to intense brown, which was observed visually, demonstrated the efficacy of *Myristica fragrans* seed extract in the biosynthesis of silver nanoparticles (Figure 1a). The synthesis of silver nanoparticles takes 20 min. The change in color in the reaction mixture strongly suggests the reduction of pure  $Ag^+$  to  $Ag^0$ . There is no rise in the strength of brown color after 2 h of incubation, indicating that  $Ag^+$  has been fully reduced.

### Characterization of AgNPs

#### UV-Visible Spectroscopy of MFHENP

The UV absorption peak appeared at 430nm in the visible range (Figure 1b). The silver nanoparticles synthesized from *Myristica fragrans* seeds extract showed a distinct peak at around 400–450nm, which confirmed the formation of AgNPs.

#### SEM with EDX Analysis of MFHENP

These SEM studies were carried out to determine the surface, size, and shape of the silver nanoparticles synthesized from the hydroethanolic extract of *Myristica fragrans* seeds. The SEM image shows that silver nanoparticles synthesized were small and polygonal in shape and their size ranges 50–60nm (Figure 1c). The formation of silver nanoparticles was verified by the EDX study, which revealed a high signal energy peak for silver atoms in the

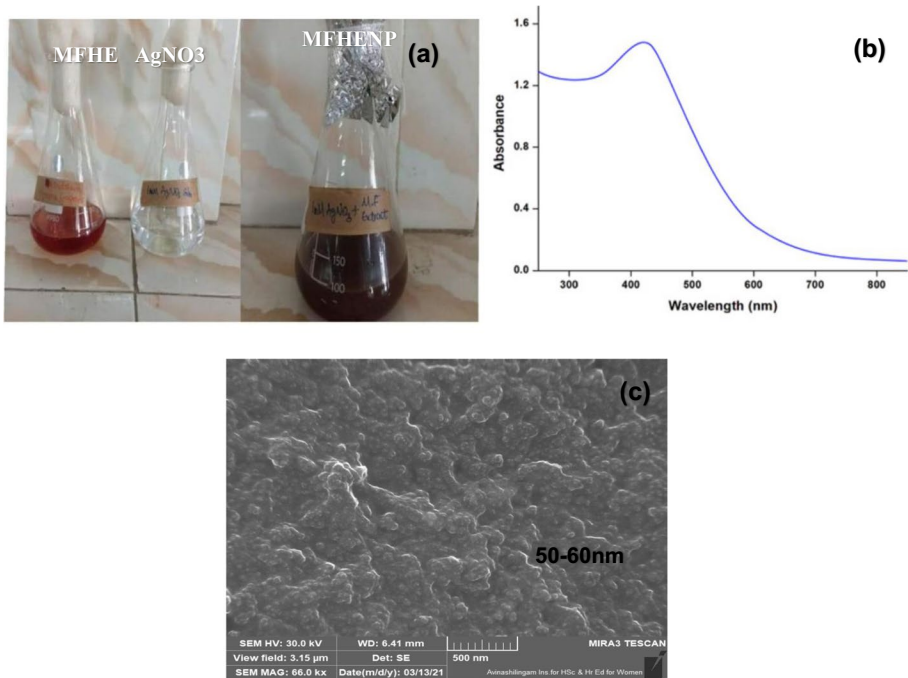


**Fig. 1** Biosynthesis of Silver nanoparticles of *Myristica fragrans* (a), UV-visible spectroscopy graph of MFHENP (b), and scanning electron microscopy (SEM) images of silver nanoparticles from hydroethanolic extract of *Myristica fragrans* (c)

range of 0.1–2.5 KeV (Figure 2b). The EDAX value confirms that the formed nanoparticle is silver. Additional peaks were discovered in the MFHENP, indicating the existence of organic and inorganic compounds.

### XRD Analysis of MFHENP

The MFHENP XRD spectra showed the existence of a significant Ag peak. The XRD pattern of MFHENP illustrated different peaks at 39°, 45°, 65°, and 78° which could be indexed to 610, 290, 220, and 210 planes of the face-centered cubic structure of AgNPs (Figure 2c). The synthesis of AgNPs of *Myristica fragrans* was confirmed with the presence of a peak at 39°. These results confirmed synthesized AgNPs are crystalline.

### FTIR Analysis of MFHE and MFHENP

The FTIR spectrum revealed the different functional groups present in the active components of MFHE and MFHENP (Figure 2d). Table 1 shows the different MFHE absorption peaks, their change in MFHENP, absorption frequency, and their corresponding functional groups. The results of FTIR analysis of MFHE and MFHENP showed N-H group stretching at 3340.71 and 3286.70 peaks. 2978.09 peak of MFHE corresponded to cyclic amines methylene groups of cycloalkanes. The peak 2893.22 of both MFHE and MFHENP corresponded to C-C methane groups of alkanes. MFHE peak 2113.98 showed bending of

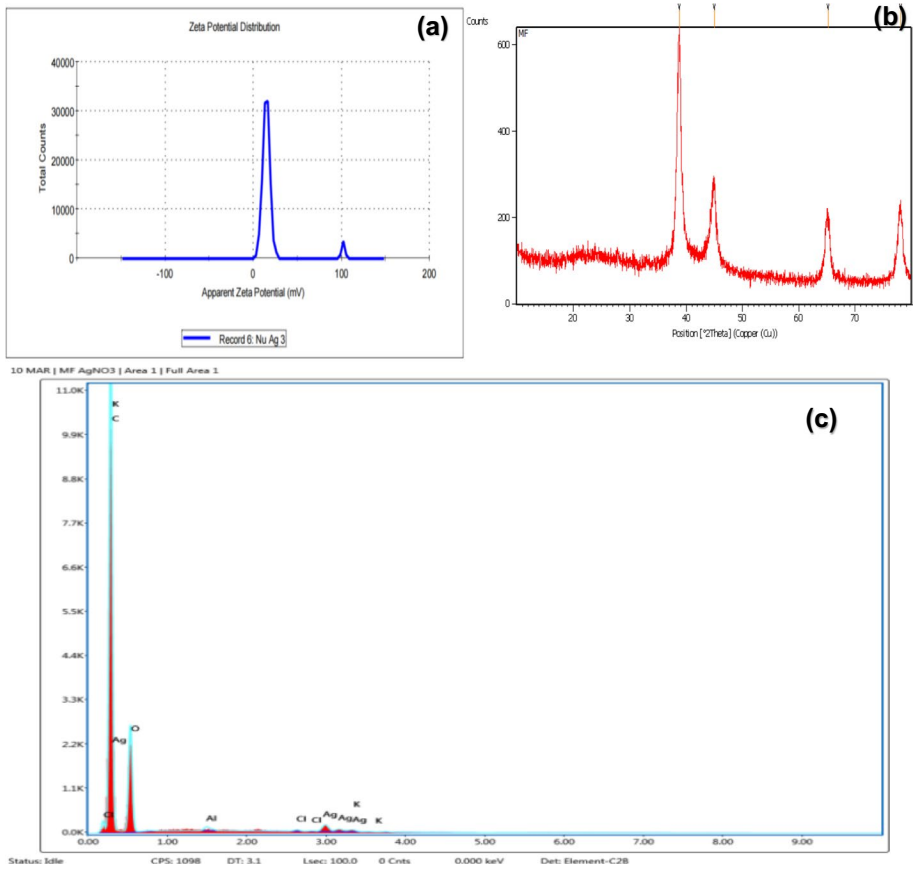


**Fig. 2** Zeta potential analysis of MFHENP (a), X-ray diffraction (XRD) analysis of MFHENP (c), energy-dispersive X-ray spectroscopy (EDX) analysis of MFHENP (b), and Fourier transform infrared spectrophotometer (FTIR) analysis of MFHENP and MFHE (d)

methane groups of alkanes. 1643.35 peak of both corresponded to C=C groups or carboxy. The 1381.03 and 1327.03 peaks of MFHE corresponded to bending of CH<sub>2</sub> group or isopropyl and C=O group of aliphatic aldehydes respectively. The peaks 1087.85 and 1080.14 of MFHE and MFHENP corresponded to bending of phenyl nucleus group of monosubstituted and final peaks 1041.56 and 1049.28 corresponded to bending of phenyl nucleus group of para-di-substituted. These findings show that in MFHE and MFHENP, amine, methane, and phenyl nucleus groups are the most abundant.

### Zeta Potential Analysis of MFHENP

The stability of MFHENP was determined using the zeta potential method. The average zeta potential was discovered to be 14mV (Figure 2a). This value was found to be within the normal range of -20 to +20. These findings revealed that MFHENP is extremely stable.

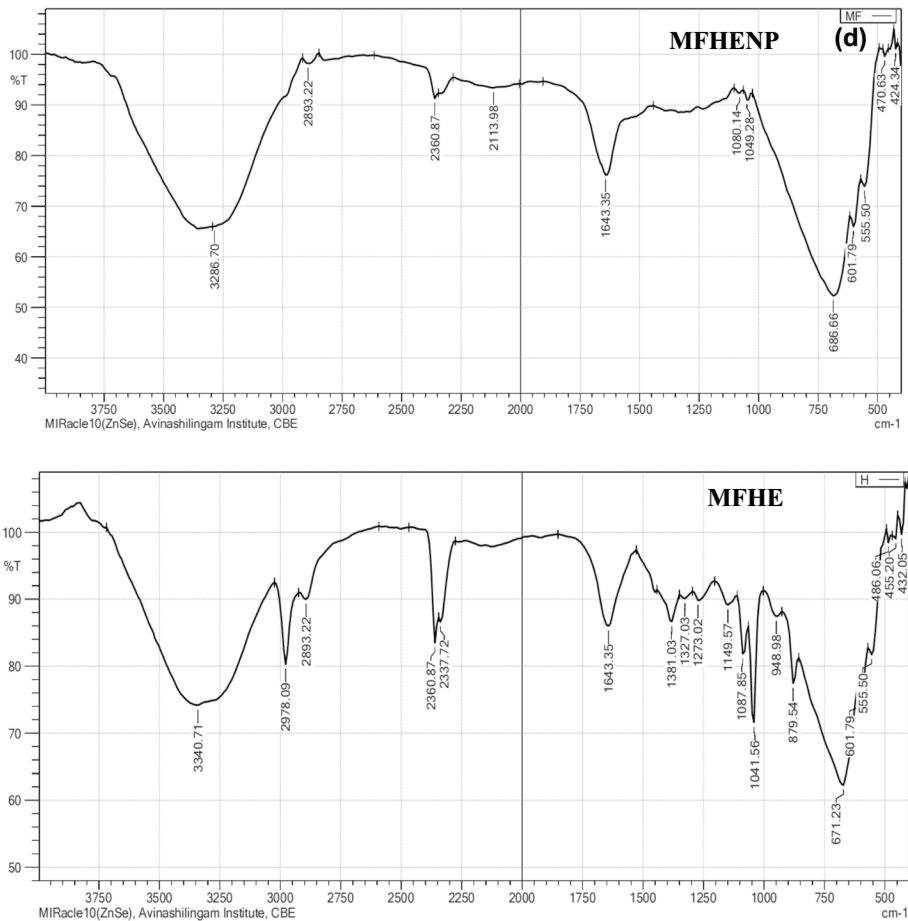


Fig. 2 (continued)

## In Vitro Anti-Diabetic Activity

### Alpha-Amylase Inhibitory Activity

Alpha-amylase ( $\alpha$ -amylase) is an intestinal enzyme that aids in the digestion of carbohydrates and the absorption of glucose. Suppressing the action of digestive enzymes like an  $\alpha$ -amylase will slow the digestion of starch and oligosaccharides, lowering glucose absorption and, as a result, blood glucose levels [25]. MFHENP was tested for  $\alpha$ -amylase inhibitory efficacy at concentrations ranging from 200 to 1000 $\mu$ g/ml (Figure 3). In a dose-dependent manner, silver nanoparticles display effective inhibitory activity against the enzyme  $\alpha$ -amylase. Synthesized silver nanoparticles from *Myristica fragrans* seeds have a  $\alpha$ -amylase inhibitory effect of 22-52%. The highest concentrations of acarbose and MFHENP (1000 $\mu$ g/ml) inhibited 59.15% percent and 52.48% respectively. Under in vitro conditions, these findings showed that MFHENP effectively inhibited the activity of the  $\alpha$ -amylase enzyme.

**Table 1** FTIR peak values, absorption frequency, and corresponding functional group of MFHE and MFHENP

S. no	Peak in MFHE $\text{cm}^{-1}$	Peak in MFHENP $\text{cm}^{-1}$	Absorption frequency $\text{cm}^{-1}$	Corresponding functional group
1.	3340.71	3286.70	3350–3010	Stretching of N-H group of secondary amines
2.	2978.09	-	$2980 \pm 5$	Stretching of Cyclic amines methylene group or cycloalkanes
3.	2893.22	2893.22	$2890 \pm 10$	Stretching of C-C methane groups of alkanes
4.	-	2113.98	2140–2100	Bending of methane groups of alkanes
5.	1643.35	1643.35	1645–1620	Stretching of C=C groups of carboxy
6.	1381.03	-	1385–1380	Bending of $\text{CH}_2$ group of Isopropyl
7.	1327.03	-	1440–1325	Stretching of C=O carbonyl group of Aliphatic aldehydes
8.	1087.85	1080.14	1110–1070	Bending of phenyl nucleus group of monosubstituted
9.	1041.56	1049.28	1070–1000	Bending of phenyl nucleus group of para-di-substituted

### Alpha-Glucosidase Inhibitory Activity

The alpha-glucosidase ( $\alpha$ -glucosidase) enzyme, which is found in the mucosal brush border of the small intestine, is also a vital digestive enzyme. Its job is to break down and process complex carbohydrates into tiny, plain, and absorbable pieces. Its inhibition is an active way to slow down glucose absorption and avoid high postprandial blood glucose levels, which can help to slow the progression of diabetes [26]. At  $\alpha$ -glucosidase concentrations of 200, 400, 600, 800, and 1000  $\mu\text{g/ml}$ , the percentage inhibition by MFHENP was increased in a concentration-dependent manner (Figure 3). The highest concentration of MFHENP and acarbose 1000  $\mu\text{g/ml}$  showed the highest inhibition of 55.6% and 71.03%. Thus, these results showed both acarbose and MFHENP have significant potential in inhibiting  $\alpha$ -glucosidase enzyme activity.

### Glucose Diffusion Assay

In this present study, the efficiency of the biosynthesized silver nanoparticles of *Myristica fragrans* seeds to inhibit the glucose movement across dialysis membrane was tested in in vitro. The silver nanoparticles effectively retarded the glucose movement across the membrane by binding to the glucose molecule (Figure 4). The absorbance of the control and MFHENP at the period of 3 h are shown in Table 2. The inhibitory action may be due to the complex formation between the glucose molecule and the components in the MFHENP. Both control and MFHENP showed potential in inhibiting the glucose movement across the membrane.

### Glucose Uptake by Yeast cells

The MFHENP was compared to the regular drug acarbose for the percentage of glucose uptake in yeast cells. In yeast cells, the rate of glucose transport across the cell

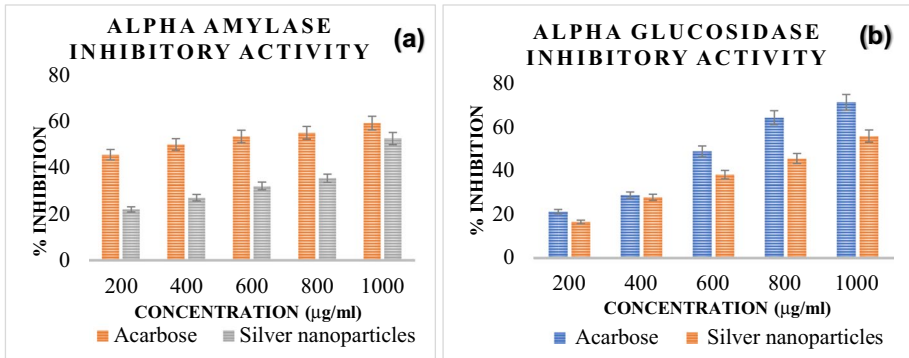


**Fig. 3** **a** Alpha-amylase inhibitory activity of MFHENP and **b** alpha-glucosidase inhibitory activity of MFHENP

membrane was investigated, and the results are showed that at higher concentrations (1000g/ml) MFHENP and acarbose displayed a percentage inhibition of 73.33% and 69.96% respectively (Figure 4). These results confirmed that acarbose and MFHENP are efficient in inhibiting the rate of glucose transport in yeast cells.

## Conclusion

This study represents green synthesis as a clean, cost-effective, and excellent method for the development of nanoparticles. The formation of MFHENP has been proven by various characterization methods. UV-visible spectroscopy reveals a peak at 430nm, SEM confirms particle size and shape, EDX spectra confirm the presence of silver ions, XRD reveals crystalline structure, FTIR identifies functional groups that serve as capping material on MFHENP, and zeta potential demonstrates stability. Furthermore, the results of this study showed that MFHENP has an inhibition effect against the enzymes  $\alpha$ -amylase and

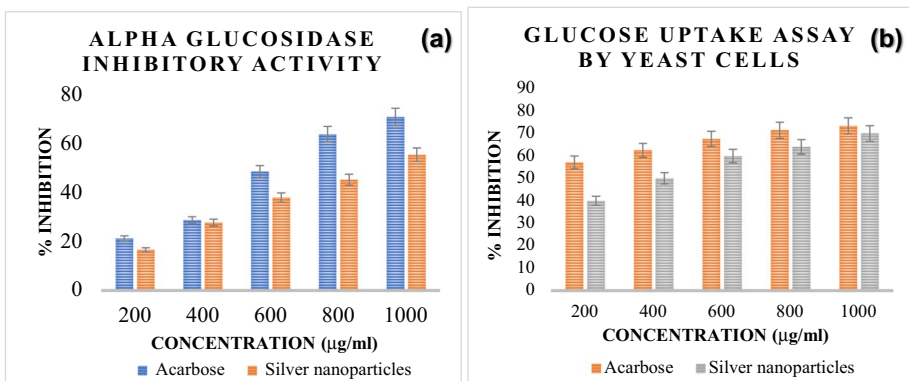


**Fig. 4** **a** Glucose diffusion assay of MFHENP and **b** glucose uptake assay of MFHENP

**Table 2** Absorbance values of MFHENP and control

Time interval (min)	Control (nm)	MFHENP (nm)
30	0.21	0.18
60	0.26	0.23
90	0.32	0.25
120	0.33	0.29
150	0.39	0.33
180	0.45	0.39

$\alpha$ -glucosidase, as well as inhibitory efficiency in glucose transport across membranes as measured by glucose diffusion and uptake assays. As a result, their efficacy in the treatment of diabetes mellitus is established. However, more in-depth studies in aspects of in vitro and in vivo procedures are required to establish MFHENP as a promising competitor for the treatment of type 2 diabetes mellitus with high therapeutic efficiency and lower side effects.

**Availability of Data And Materials** All data generated or analyzed during this study are included in this published article [and its supplementary information files].

The datasets generated during and/or analyzed during the current study are available from the corresponding author on reasonable request.

**Author Contribution** RP contributed to the data collection, data analysis and interpretation, article drafting, and critical revision of the article. LK contributed to the design of work and article finalization.

## Declarations

**Ethical Approval** Not applicable

**Consent to Participate** Not applicable

**Consent for Publication** Not applicable

**Conflict of Interest** The authors declare no competing interests.

## References

1. Bayda, S., Adeel, M., Tuccinardi, T., Cordani, M., & Flavio Rizzolio, F. (2020). *The history of nanoscience and nanotechnology: from chemical–physical applications to nanomedicine, molecules*, 25, 1–15.
2. Almatroudi, A. (2020). Silver nanoparticles: synthesis, characterisation and biomedical applications. *Open Life Sciences*, 15, 819–839. <https://doi.org/10.1515/biol-2020-0094>
3. Dawadi, S., Katuwal, S., Gupta, A., Lamichhane, U., Thapa, R., Jaisi, S., Lamichhane, G., Bhattarai, D. P., & Parajuli, N. (2021). Current research on silver nanoparticles: synthesis, characterization, and applications. *Journal of nanomaterials*, 1–23.
4. He, Y., Al-Mureish, A., & Wu, N. (2021). Nanotechnology in the treatment of diabetic complications: a comprehensive narrative review. *Journal of Diabetes Research*, 1–11. <https://doi.org/10.1155/2021/6612063>
5. Mikhailova, E. O. (2020). Silver nanoparticles : mechanism of action and probable bio application. *Journal of functional biomaterials*, 1–26. <https://doi.org/10.3390/jfb11040084>
6. Diabetes-overview, symptoms and treatments, World Health Organization, 2021.

7. Diabetes, World Health Organization, (2021).
8. Adnette, F. N., Ulbad, T. P., Magloire, N., Ruffine, F., Koutinhouin, G. B., & Akadir, Y. (2019). Diabetes mellitus: classification epidermiology, physiopathology, immunology, risk factors, prevention and nutrition. *International journal of advanced research*, 7, 855–863. <https://doi.org/10.21474/IJAR01/9433>
9. Padhi, S., Nayak, A. K., & Behera, A. (2020). Type II diabetes mellitus: a review on recent drug-based therapeutics. *Biomedical and Pharmacotherapy*, 131, 1–23. <https://doi.org/10.1016/j.biopha.2020.110708>
10. Tran, N., Pham, B., & Le, L. (2020). Bioactive compounds in anti-diabetic plants: from herbal medicine to modern drug discovery. *Biology*, 9, 1–31. <https://doi.org/10.3390/biology9090252>
11. Liyanagamage, D. S. N. K., Jayasinghe, S., Attanayake, A. P. and Karunaratne, V., (2020) Medicinal plants in management of diabetes mellitus: an overview, *Ceylon Journal of Science*, 49: 03-11. DOI: <http://doi.org/10.4038/cjs.v49i1.7700>
12. Gupta, E. (2020). Elucidating the phytochemical and pharmacological potential of *Myristica fragrans* (Nutmeg). *Researchgate*. <https://doi.org/10.4018/978-1-7998-2524-1.ch004>
13. Ha, M. T., Vu, N. K., Tran, T. H., Kim, J. A., Wool, M. H., & Min, B. S. (2020). Phytochemical and pharmacological properties of *Myristica fragrans* Hoult.: an updated review. *Activities of Pharmacol research*, 1–36. <https://doi.org/10.1007/s12272-020-01285-4>
14. Donda, M. R., Kudlea, K. R., Alwalaa, J., Miryalaa, A., Sreedharb, B., & Rudraa, M. P. P. (2013). Synthesis of silver nanoparticles using extracts of *Securiniga leucopyrus* and evaluation of its antibacterial activity. *International Journal of Current science and research*, 7, 1–8.
15. Sulaiman, G. M., Mohammed, W. H., Marzoog, T. R., Al-Amiery, A. A. A., Kadhum, A. A. H., & Mohamad, A. B. (2013). Green synthesis, antimicrobial and cytotoxic effects of silver nanoparticles using *Eucalyptus chapmaniana* leaves extract. *Asian Pacific Journal of Tropical Biomedicine*, 3, 58–63.
16. Das, G., Patra, J. K., Debnath, T., Ansari, A. and Shin, H. S., (2019) Investigation of antioxidant, antibacterial, antidiabetic, and cytotoxicity potential of silver nanoparticles synthesized using the outer peel extract of *Ananas comosus* (L.), 1-19.
17. Patra, J. K., Das, G., Kumar, A., Ansari, A., Kim, H., & Shin, H. S. (2018). Photo-mediated biosynthesis of silver nanoparticles using the non-edible accrescent fruiting calyx of *Physalis peruviana* L. fruits and investigation of its radical scavenging potential and cytotoxicity activities. *Journal of Photochemistry and Photobiology B: Biology*, 188, 116–125.
18. Venil, K., Malathi, M., Velmurugan, P., & Devi, P. R. (2020). Green synthesis of silver nanoparticles using canthaxanthin from *Dietzia maris* AURCCBT01 and their cytotoxic properties against human keratinocyte cell line Chidambaram. *Journal of applied microbiology*, 1–36. <https://doi.org/10.1111/jam.14889>
19. Ahamad, I., Aziz, N., Zaki, A., & Fatma, T. (2021). Synthesis and characterization of silver nanoparticles using *Anabaena variabilis* as a potential antimicrobial agent. *Journal of Applied Phycology*, 1–15. <https://doi.org/10.1007/s10811-020-02323-w>
20. Vitthal, K. H. (2013). Study of solid lipid nanoparticles as a carrier for bacoside. *International Journal of Pharmacy and Biological Sciences*, 3, 414–426.
21. Bagyalakshmi, J., & Haritha, H. (2021). Green synthesis and characterization of silver nanoparticles using *Pterocarpus marsupium* and assessment of its *in-vitro* antidiabetic activity. *American Journal of Advanced drug delivery*, 1–7.
22. Govindappa, M., Hemashekhar, B., Manoj-Kumar, A., Ravishankar Rai, V., & Ramachandra, Y. L. (2018). Characterization, antibacterial, antioxidant, antidiabetic, anti-inflammatory and antityrosinase activity of green synthesized silver nanoparticles using *Calophyllum tomentosum* leaves extract. *Results in Physics*, 9, 400–408. <https://doi.org/10.1016/j.rinp.2018.02.049>
23. Vani, M., Vasavi, T., & Devi, U. M. P. (2018). Evaluation of *in-vitro* antidiabetic activity of methanolic extract of *Seagrass halophila beccarii*. *Asian journal of pharmaceutical and clinical research*, 11, 150–153.
24. Abubakar, A. N., Lawal, Z. B., Japeth, E., Yunus, I. O. and Garba, R., (2021) *In vitro* antidiabetic potentials of crude saponins extract from *Leptodenia hastata* and *Adansonia digitata* leaves, *GSC advanced research and reviews*, 2021; 6: 61-66. .
25. Shettar, A. K., Sateesh, M. K., Kaliwal, B. B. and Vedamurthy, A. B., (2017) *In vitro* antidiabetic activities and GC-MS phytochemical analysis of *Ximenia americana* extracts, *South African Journal of Botany*, 111: 202-211. Doi: 10.1016/j.sajb.2017.03.014

26. Mechchate, H., Es-safi, I., Louba, A., Alqahtani, A. S., Nasr, F. A., Noman, O. M., Farooq, M., Alharbi, M. S., Alqahtani, A., Bari, A., Bekkari, H. and Bousta, D., (2021) *In vitro* alpha-amylase and alpha-glucosidase inhibitory activity and *in vivo* antidiabetic activity of *Withania frutescens* L. foliar extract, *Molecules*, 26: 1-30. Doi: 10.3390/molecules26020293

**Publisher's Note** Springer Nature remains neutral with regard to jurisdictional claims in published maps and institutional affiliations.